

A Unity Power Factor Buck Pre-Regulator with Feedforward of the Output Inductor Current

Fabiana Pöttker de Souza and Ivo Barbi

Federal University of Santa Catarina
Department of Electrical Engineering
Power Electronics Institute

P. O. BOX 5119 – 88040-970 – Florianópolis – SC - Brazil
Phone: 55-48-331.9204 – FAX: 55-48-234.5422 – E-mail: fabiana@inep.ufsc.br
Internet: <http://www.inep.ufsc.br>

Abstract - This paper presents a new technique to get unity power factor in a single-phase rectifier based on a Buck pre-regulator. The proposed control technique, which employs a feedforward of the output inductor current, allows the use of a small low frequency inductor with a high current ripple. Theoretical analysis, design procedure and experimental results of a 750W, 30kHz prototype are presented in the paper.

I. INTRODUCTION

The Buck pre-regulator presented in Fig. 1 has some important characteristics such as the absence of inrush current, low DC output voltage, protection against short circuit, among others.

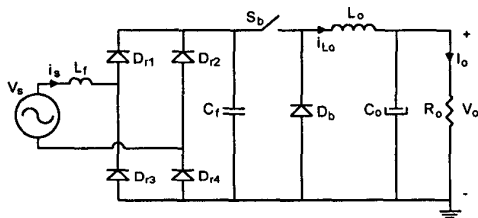


Fig. 1 – The Buck pre-regulator.

In discontinuous conduction mode [1], with a high frequency output inductor L_o , the input current is zero while the instantaneous value of the input voltage is smaller than the output voltage. The input current harmonic distortion is dependent on the ratio between the output voltage average value and the input voltage peak value. Fig. 2 shows the simulation results for an inductance L_o of 95 μ H. Depending on the design, the third and the fifth harmonic components may not be in compliance with IEC 1000-3-2 [2]. Another disadvantage of the discontinuous conduction mode is that the peak and rms currents are very high, leading to high conduction losses in the switches.

On the other hand, in continuous conduction mode, with a low frequency output inductor designed in such a way that it behaves as a constant current source, the problem stated above no longer exists. However the size and weight in this case is much bigger. The employed control technique is presented in Fig. 3. The output voltage is sensor and compared to a reference voltage. The resulting error is injected in an appropriate voltage controller. A sensor of the rectified input voltage multiplies the voltage controller output

signal. The resulting modulation signal is compared with the saw-tooth signal, generating the drive signal to the switch S_b . In Fig. 4 it is presented the simulation results employing this control strategy, for an inductance L_o of 1H. As it can be noticed the input current is practically sinusoidal and a high power factor is achieved.

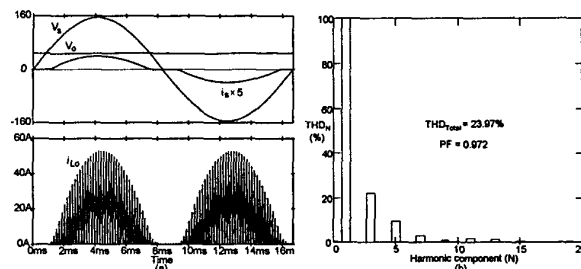


Fig. 2 – Discontinuous conduction mode simulation results.

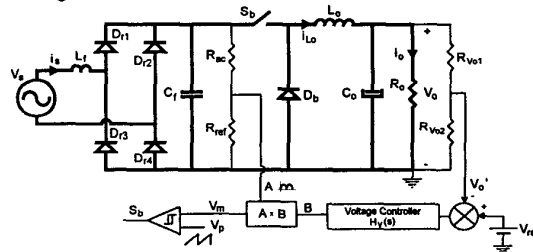


Fig. 3 – The Buck pre-regulator control diagram for continuous conduction mode.

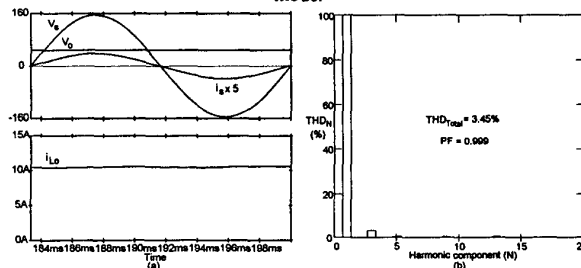


Fig. 4 – Continuous conduction mode simulation results for an inductance L_o of 1H.

In order to optimize the size and weight, the inductance L_o may be decreased, so it no longer behaves as a constant current source. Although, increasing the output inductor current ripple distorts the input current, with a significant third harmonic component, as shown in the simulation results of Fig. 5, for an inductance L_o of 15mH.

Reference [3] proposes a control technique to eliminate the distortion of the input current even when the output inductor current presents a large ripple. The difference between this technique and the one presented in Fig. 3 is that the modulation signal is compared to a saw-tooth whose peak value is proportional to the current i_{L_o} . The current i_{L_o} is detected and fed into an integrator circuit, which is reset at a constant interval and its output is the saw-tooth whose peak value is proportional to the inductor current.

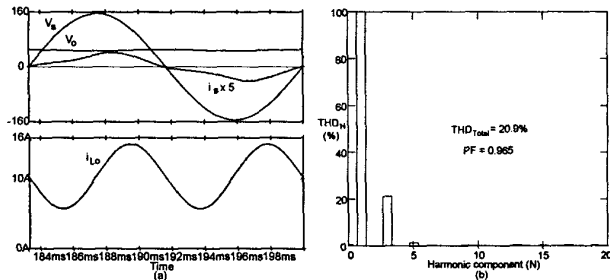


Fig. 5 – Continuous conduction mode simulation results for an inductance L_o of 15mH.

The feedforward of the output inductor current presented in this work also compensates the ripple in the output inductor current, however, on a different way. The difference between the proposed technique and the one presented by [3] is that the information about the output inductor current is on the modulation signal instead of being in the saw-tooth. The authors believe that this is an easier way to implement this technique.

With a technique to compensate the output inductor current ripple one could think to increase the ripple until the size and weight are appropriate for a certain application. However, there is a limit. This limit and another important issues are presented in the theoretical analysis of Section III.

II. CONTROL STRATEGY

The buck pre-regulator with feedforward of the output inductor current is presented in Fig. 6. The output voltage is sensor and compared to a reference voltage. The resulting error is injected in an appropriate voltage controller. The output of the voltage controller is multiplied by a sensor of the rectified input voltage and divided by a sensor of the current in the output inductor. The resulting modulation signal is compared with the saw-tooth signal, generating the drive signal to the switch S_b .

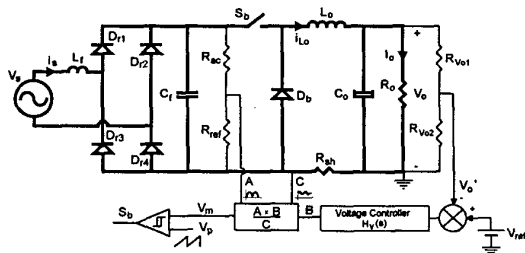


Fig. 6 – Buck pre-regulator with the proposed control strategy.

In Fig. 7 are presented the output inductor current and the resulting modulation signal. Thanks to the feedforward strategy the modulation signal presents a distortion that eliminates the input current distortion due to the output inductor current ripple. In Fig. 7 it is also presented the saw-tooth signal being compared to the modulation signal and the resulting drive signal to the switch S_b .

Without the feedforward technique there is no information about the current in the output inductor, so the modulation signal, obtained by the multiplication of “A” and “B”, results in a sinusoidal signal.

In Fig. 8 it is presented the simulation results employing the proposed control strategy, for the same specifications of the simulation results presented in Fig. 5. As it can be noticed the third harmonic was almost eliminated, resulting in a high power factor.

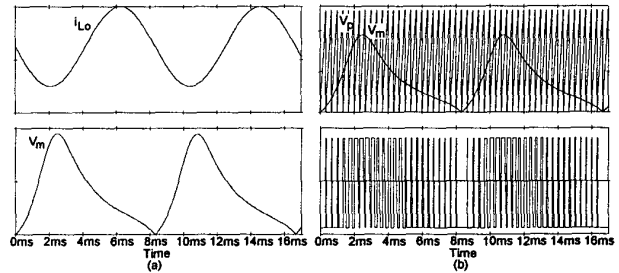


Fig. 7 – Simulation results of the proposed control strategy for a low switching frequency.

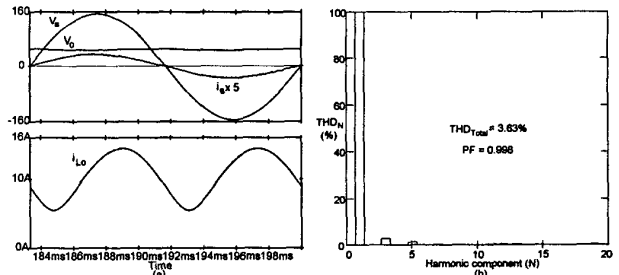


Fig. 8 – Simulation results of the proposed control strategy for an inductance L_o of 15mH

III. THEORETICAL ANALYSIS

A. Output Inductor Current Ripple Limit

In a buck converter the output current is bigger than the input current. The limit for the output inductor current ripple is the one that guarantees that the output inductor current equals the input current in one point only, as shown in Fig. 9 (a). Otherwise the input current will be distorted, as shown in Fig. 9 (b). Equation (1) and (2) define the input and output inductor currents.

$$i_s(\theta) = i_{s\ peak} \sin(\theta) \quad (1)$$

$$i_{L_o}(\theta) = I_o - \frac{\Delta I_o}{2} \sin(2\theta) \quad (2)$$

In order to find out the maximum output inductor current ripple, (1) and (2) are made equal, resulting in (3).

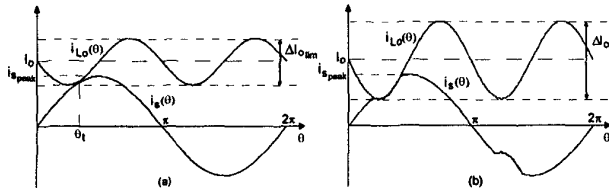


Fig. 9 – (a) Output inductor current ripple limit, (b) beyond the output inductor current ripple limit.

$$\Delta I_{or} = 2 (1 - M_i \sin(\theta)) / \sin(2\theta) \quad (3)$$

Where: $M_i \rightarrow$ modulation index ($M_i = i_{s \text{ peak}} / I_o$).

$\Delta I_{or} \rightarrow$ relative ripple ($\Delta I_{or} = \Delta I_o / I_o$).

In order to obtain the angle θ , where the currents touch each other in one point, (3) is derived and made equal to zero, as shown in (4). Solving (4) algebraically the angle θ is obtained as a function of the modulation index, as shown in Fig. 10. The currents will touch in one point always between 45° and 90° . Substituting the angle θ in (3) the maximum relative current ripple is obtained as a function of the modulation index, as shown in Fig 11.

$$\frac{d\Delta I_{or}}{d\theta} = \frac{2 (-\sin(2\theta) M_i \cos(\theta) - 2 (1 - M_i \sin(\theta) \cos(2\theta)))}{[\sin(2\theta)]^2} = 0 \quad (4)$$

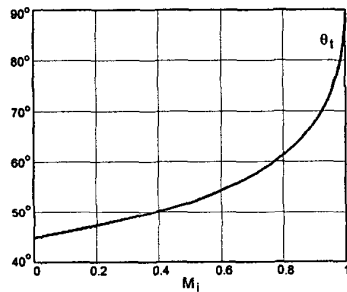


Fig. 10 – Angle θ , in which the currents touch in one point.

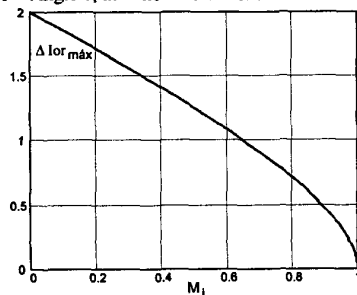


Fig. 11 –Maximum relative ripple.

B. Output Characteristics

The average output voltage without the feedforward control technique is represented by (5), and with the feedforward control technique is represented by (6). The output characteristics are presented in Figs. 12 and 13. As can be noticed, with the feedforward control technique the average output voltage is dependent on the output current,

and without the feedforward control technique the average output voltage is independent of the output current.

$$\overline{V_o} = \frac{V_o \text{ avg}}{V_s \text{ peak}} = \frac{M_i}{2} \quad (5)$$

$$\overline{V_o} = \frac{V_o \text{ avg}}{V_s \text{ peak}} = \frac{\overline{V_m}}{2 I_o} \quad (6)$$

Where: $\overline{V_m} = V_m / V_{m \text{ max}}$, $\overline{I_o} = R_{sh} I_o / V_{m \text{ max}}$.

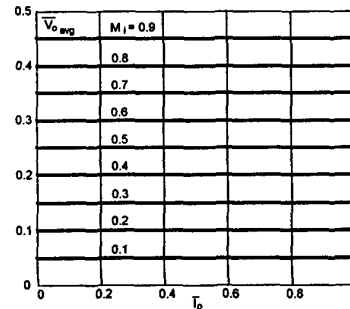


Fig. 12 – Output characteristics without the feedforward control technique.

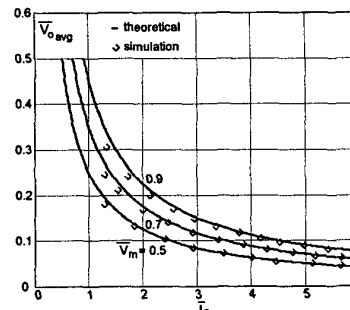


Fig. 13 – Output characteristics with the feedforward control technique.

Equation (7) presents the transfer function of the output voltage versus the output inductor current. The voltage controller is presented in Fig. 14 and its transfer function in (8).

$$G_v(s) = \frac{V_o(s)}{i_{Lo}(s)} = \frac{R_o}{(1 + s C_o R_o)} \quad (7)$$

$$H_v(s) = \frac{V_o'(s)}{V_c(s)} = \frac{-(1 + s R_2 C_1)}{s C_1 R_1} \quad (8)$$

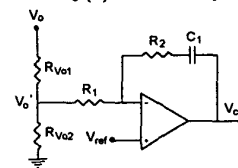


Fig. 14 – Voltage controller.

IV. DESIGN METHODOLOGY AND EXAMPLE

A simplified design procedure and example is described in this section, according to the analysis presented in Section III. The specifications are as follows:

$$V_s = 311V, f_{line} = 60Hz, P_{o\,nom} = 1.5kW, f_s = 30kHz,$$

$$P_{o\,min} = 0.5 \times P_{o\,nom} = 750W, I_{o\,nom} = 25A,$$

$$I_{o\,min} = 12.5A, V_o = 60V, \Delta V_o = 10\% \times V_o = 6V.$$

The input current for nominal and minimum power, and the modulation index are calculated.

$$i_{s\,peak\,nom} = \frac{2 P_{o\,nom}}{V_{s\,peak}} = \frac{2 \times 1500}{311} = 9.65 A$$

$$i_{s\,peak\,min} = \frac{2 P_{o\,min}}{V_{s\,peak}} = \frac{2 \times 750}{311} = 4.82 A$$

$$M_i = \frac{i_{s\,peak\,nom}}{I_{o\,nom}} = \frac{i_{s\,peak\,min}}{I_{o\,min}} = \frac{9.65}{25} = 0.386$$

The maximum relative output inductor current ripple is calculated as shown below.

$$\frac{d\Delta I_{or}}{d\theta} = \frac{d}{d\theta} \left(2 \frac{1 - M_i \sin(\theta)}{\sin(2\theta)} \right) = 0 \Rightarrow \theta_t$$

$$\theta_t = 50^\circ$$

$$\Delta I_{or\,max} = 2 \left(\frac{1 - M_i \sin(\theta_t)}{\sin(2\theta_t)} \right) = 2 \times \left(\frac{1 - 0.386 \times \sin(50^\circ)}{\sin(2 \times 50^\circ)} \right) = 143\%$$

The maximum relative ripple shall occur in the minimum power, so the absolute output current ripple is calculated.

$$\Delta I_o = \Delta I_{or\,max} \times I_{o\,min} = 1.43 \times 12.5 = 17.9 A$$

Once the output inductor current ripple and the output voltage ripple are defined, the inductance L_o and capacitance C_o are calculated.

$$L_o = \frac{P_{o\,nom}}{2 \pi f_{line} I_o \Delta I_o} = \frac{1500}{2 \times \pi \times 60 \times 25 \times 17.9} = 8.9mH$$

$$C_o = \frac{\Delta I_o}{4 \pi f_{line} \Delta V_o} = \frac{17.8}{4 \times \pi \times 60 \times 6} = 3.93mF \Rightarrow 4.3mF$$

The capacitor C_o rms current is calculated as follows:

$$i_{C_{o\,ef}} = \frac{\Delta I_o}{2\sqrt{2}} = \frac{17.9}{2\sqrt{2}} = 6.33 A$$

The high frequency input filter (L_f and C_f) is calculated according to the following procedure.

$$f_c = \frac{f_s}{10} = 3kHz \Rightarrow \omega_c = 18850 rad/s$$

$$\zeta = 1.0$$

$$R_{eq} = \frac{V_{s\,peak}}{i_{s\,peak\,nom}} = \frac{311}{9.65} = 32.24\Omega$$

$$C_f = \frac{1}{R_{eq} 2 \zeta \omega_c} = \frac{1}{32.24 \times 2 \times 1 \times 18850} \cong 0.8\mu F$$

$$L_f = \frac{1}{\omega_c^2 C_f} = \frac{1}{18850^2 \times 0.8\mu} \cong 3.5mH$$

$$\text{Adjusting the filter by simulation: } \begin{cases} C_f = 2\mu F \\ L_f = 1.4mH \end{cases}$$

The $G_v(s)$ transfer function is calculated as shown below.

$$G_v(s) = \frac{R_{o\,nom}}{1 + s C_o R_{o\,nom}} = \frac{2.4}{1 + s 126.26}$$

The pole occurs approximately in 126rad/sec. The compensator zero shall occur near the pole so that they cancel each other. Choosing $R_1 = 67k\Omega$ and $R_2 = 33k\Omega$, C_1 is calculated.

$$C_1 = \frac{1}{126 \times 33 \times 10^3} = 240nF \Rightarrow C_1 = 220nF$$

$$H_v(s) = k_{V_o} \frac{1 + s R_2 C_1}{s R_1 C_1} = 50 \cdot 10^{-3} \frac{1 + s 137.74}{s 0.01474}$$

The Bode diagram of $G_v(s)$, $H_v(s)$ and the open loop transfer function are presented in Fig. 15. The crossover frequency is about 1.5Hz.

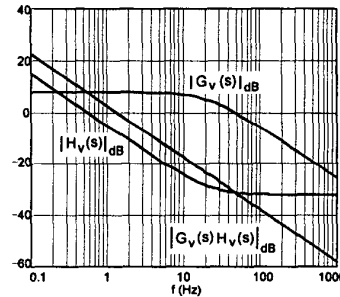


Fig. 15- Bode diagram of $G_v(s)$, $H_v(s)$ and $G_v(s)H_v(s)$.

V. EXPERIMENTAL RESULTS

In order to verify the principle of operation and the control strategy, a 750W, 30kHz prototype was built. The inductance L_o was designed to have a current ripple a little smaller than the output inductor current ripple limit. In order to implement the feedforward, multiplying A and B and dividing by C, two dedicated integrated circuit UC3854 [4] were used, as shown in Fig. 16. The specifications are as follows:

$$V_s = 220V_{rms} \quad f_{line} = 60Hz \quad V_o = 60V \quad P_o = 750W$$

$$L_f = 1.4mH \text{ (2.8cm Fe Si core, 42 turns, } 2 \times 14AWG, \text{ gap} = 0.28mm)$$

$$C_f = 2\mu F / 280V \text{ (polypropylen)}, \quad C_o = 2 \times (4.3mF, 75V)$$

$$L_o = 8.9mH \text{ (6cm Fe Si core, 63 turns, } 5 \times 12AWG, \text{ gap} = 0.24cm)$$

$$L_s = 3.4\mu H \text{ (EE 30/7 core, 5 turns, } 13 \times 19AWG)$$

$$C_s = 100nF, \quad S_b: IRG4PC50U, \quad D_b: APT30D100BN$$

In Fig. 17 it is presented the complete diagram of the implemented prototype. A passive non-dissipative snubber [5] is used as shown in the shadow areas of Fig. 17. The

inductor L_s is responsible for the “lagging effect” in the reverse recovery of diode D_b , reducing the turn on losses of switch S_b .

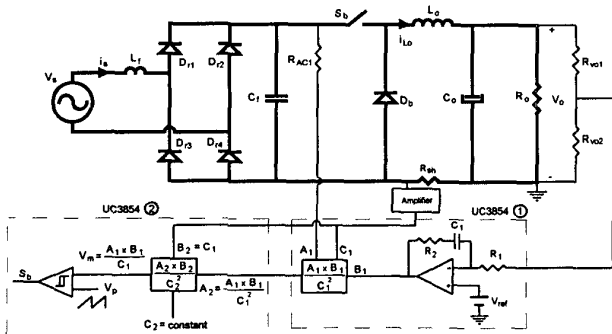


Fig. 16 – Block diagram of the implemented prototype.

The input voltage and current and the input current harmonic spectrum, without the feedforward technique, are shown in Fig. 20. The power factor decreased to 0.948 and the third harmonic is significant. In Fig. 19 (c) and 20 (c) it is presented the modulation signal with and without the feedforward strategy. It is verified that without the

feedforward strategy the modulation signal is sinusoidal, and with the feedforward strategy there is a distortion due to the output inductor current ripple.

In Fig. 21 it is presented the input voltage and current and the input current harmonic spectrum, with the feedforward technique a little beyond the output inductor current ripple. The power factor decreased to 0.994. The design shall be made to reach the output inductor current ripple limit on a “critical power”. Therefore, for a power smaller than the critical, the input current will be distorted as shown in Fig. 21, and for a power bigger than the critical, the power factor will be close to unity.

In Fig. 18 it is presented the input voltage and current and the input current harmonic spectrum. The total harmonic distortion is 5.39% and the current displacement is 1.72° resulting in a power factor of 0.998. The input voltage presented a total harmonic distortion of 2.87%. In Fig. 19 it is shown the output inductor current and the input current. As expected, the output inductor current ripple is a little smaller than the output inductor current ripple limit.

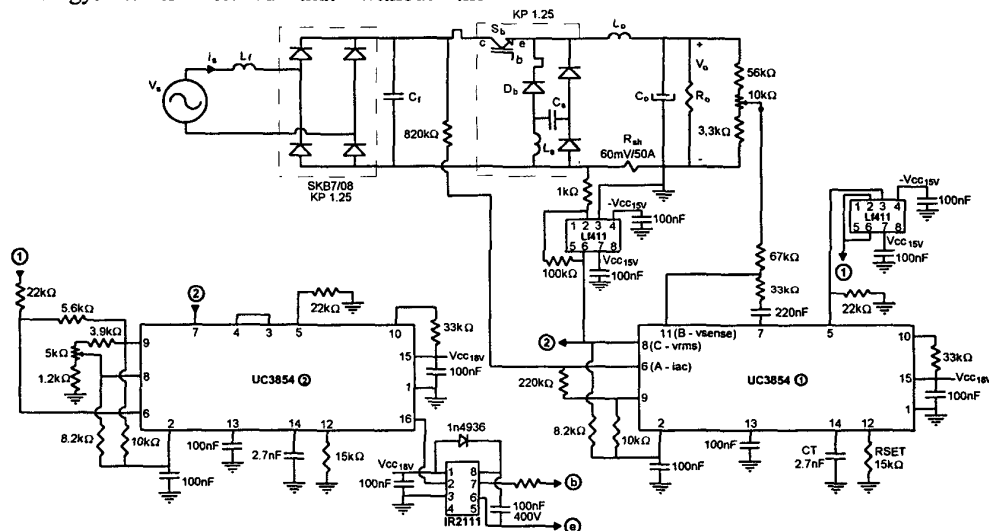


Fig. 17 – Complete diagram of the implemented prototype.

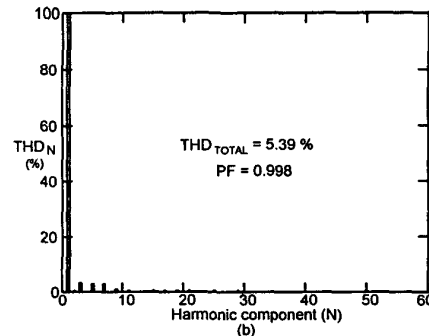
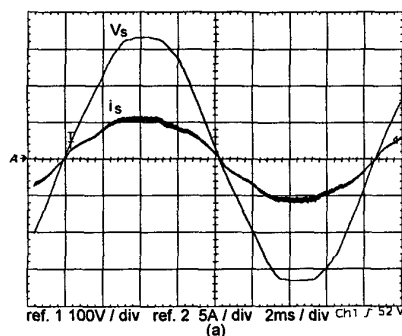


Fig. 18 – (a) Input voltage and current and (b) input current harmonic spectrum, with the feedforward technique

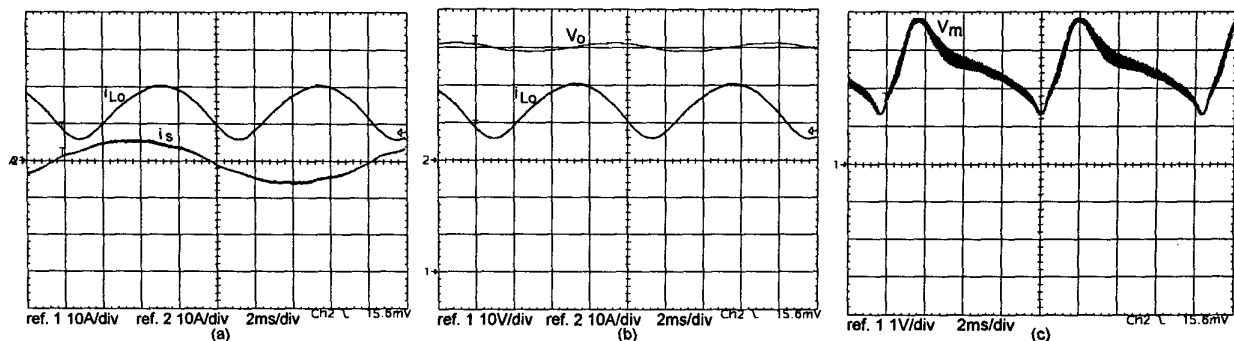


Fig. 19 – (a) Output inductor and input currents, (b) output voltage and inductor current and (c) modulation signal, with the feedforward technique.

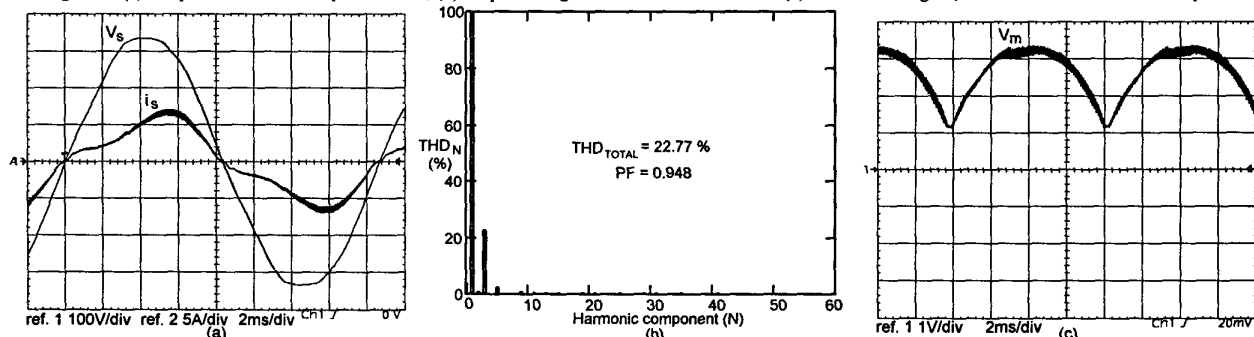


Fig. 20 – (a) Input voltage and current, (b) input current harmonic spectrum and (c) modulation signal, without the feedforward technique.

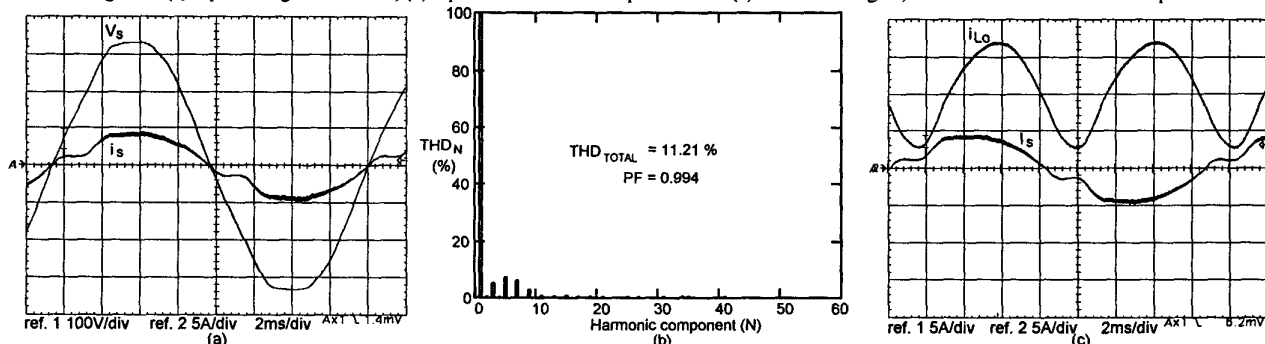


Fig. 21 – (a) Input voltage and current, (b) input current harmonic spectrum and (c) output inductor and input currents, with the feedforward technique beyond the output inductor current ripple limit.

VI. CONCLUSION

In this paper it is presented and studied a control strategy to reduce the size, weigh and cost of a Buck based unity power factor single-phase rectifier, operating in continuous conduction mode.

From these studies, the following conclusions are drawn:

- The power factor is independent on the relation between the output voltage average value and the input voltage peak value.
- Despite the utilization of a “small” filter inductor and a high 120Hz current ripple, the power factor is close to unity.
- The practical implementation is easy, with the utilization of a well-known dedicated integrated circuit (UC3854).

REFERENCES

- [1] H. Endo, T. Yamashita, T. Sigiura, “A high-power-factor Buck converter”, IEEE PESC Records, pp. 1071-1076, 1992, Toledo, Spain.
- [2] IEC, IEC 1000-3-2 Standard, International Eletrotechnic Commission, 1995, Geneve, Switzerland.
- [3] K. Hirachi, T. Iwade, K. Shibayama, “A specific control implementation on Buck-type active power filtering converters”, IEEE INTELEC Records, pp. 444-449, 1995.
- [4] C. S. Silva, “Power factor correction with UC3854”, Unित्रode Application Note U-125, 1990, Merrimack, NH, EUA.
- [5] D. Tardiff, T. H. Barton, “A summary of resonant snubber circuits for transistors and GTOs”, IEEE IAS Records, pp. 1176-1180, 1989.